Hypervelocity Impact of Small Right Circular Cylinders

W. G. Reinecke* and W. L. McKay†
Avco Space Systems Division, Wilmington, Mass.

An experimental investigation of the hypervelocity impact of two small right circular cylinders is described, one cylinder being much smaller in diameter than the other. The impact speed is 19,000 fps and the effects of various cylinder sizes and materials are assessed. All tests were conducted with the axes of the two cylinders perpendicular to each other and to the velocity vector. A light gas gun was employed to launch the cylinders. The experimental facility is described along with the development of launching techniques. The data showing the effects of material density are correlated in a form commonly used for hypervelocity data involving spheres impacting semi-infinite targets. In addition, it is shown that the mass per unit length of the minimum diameter smaller cylinder which will cut the larger rod upon impact is independent of the material properties of the smaller cylinder.

Introduction

THE problem under consideration is the hypervelocity impact of a pair of small right circular cylinders of dissimilar material and radius. The cylinders or rods have lengths that are large compared to their radii and have a relative velocity normal to both their axes. One of the rods has a radius substantially smaller (by about a factor of 10) than the other. In particular, we wished to determine just how small the smaller of the two rods could be and still completely cut the larger rod. The experiments have been restricted to the case in which the axes of the two rods were perpendicular at impact. The phenomenon is sketched in Fig. 1.

We shall correlate the effects of rod densities on the basis of a projectile hitting a large or semi-infinite target. The correlation model is shown in Fig. 2, where A is the diameter of an impacting sphere and B is the depth of the crater it causes in the target material. We associate these two dimensions, respectively, with the diameter of the smaller rod and the diameter of the largest rod it can cut. Our purpose, then, is to determine experimentally the relation between A, B, and the rod materials.

Several theories and correlations have been suggested to predict the cratering due to hypervelocity impact.[1–7] Each of the suggested formulas relates the ratio B/A to the properties of the target material and to the density and speed of the projectile. The numerical calculations of Bjork[2] are probably the best available theoretical results. However, his solutions are not available for the materials of interest here. Thus we shall of necessity employ a simple semi-empirical formula of the form

$$B/A = K(D/W)^J(u/a)^{2/3} \quad (1)$$

where A = the projectile diameter, B = the crater depth, D = the projectile density, W = the target density, u = the projectile speed, and a = the dilatational wave speed in the target. The value of K is about two[5,7] and J varies between $\frac{1}{3}$ and $\frac{2}{3}$.[4,5,7] We note at this point that these relations will probably predict too small a value for B/A when applied to the two rod problem. This is because the mass and kinetic energy involved in the impact of the real rod of diameter A will be greater than a sphere of that diameter. Moreover, the target rod is clearly not infinite in depth as assumed in the model. Thus, the purpose of the experiment was to determine J and K. Since the tests were conducted at one speed and since the speed of sound in the targets did not vary greatly, no attempt was made to determine the u/a dependence.

Test Facility

A ballistic range technique was developed to study the hypervelocity impact of two slender rods as shown in Fig. 1. The tests were performed in the Range II facility of the Avco Space Systems Division ballistics range complex (Fig. 3). The range test section is approximately 100 ft long; however, only the first 30 ft were required for these tests. The facility is equipped with a two stage, hydrogen driven, caliber 0.600 light gas gun, which is capable of launching a 3-g payload at velocities up to 23,000 fps. The test sec-

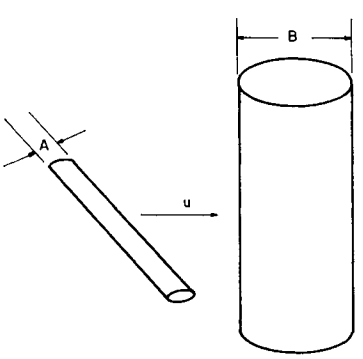

Fig. 1 Diagram showing frame of reference and orientation at impact.

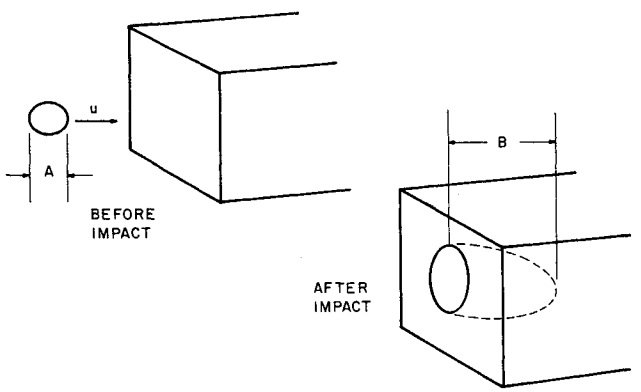

Fig. 2 Diagram showing analogous impact in semi-infinite target.

Received January 23, 1968; revision received April 17, 1969.
* Chief, Experimental Fluid Physics Section.
† Senior Staff Scientist.

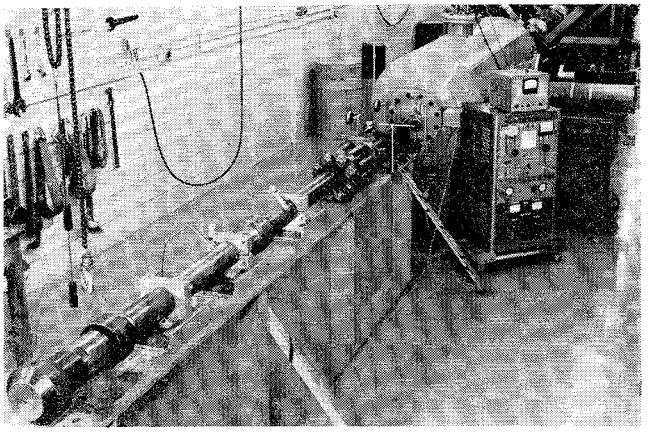

Fig. 3 Photograph of Range II facility.

tion was instrumented as shown in Fig. 4, to provide a means of photographing the event shortly after impact.

Prior to firing, a parallel network of the smaller diameter rods was mounted on a metal frame which was placed in the test section at a position 3 ft from the end of the gun barrel and aligned to intercept the larger rod. The network of smaller rods covered a 3-in.-diam circle with a $\frac{1}{4}$-in. spacing to insure intercept with the large rod, which is $\frac{1}{2}$ in. long.

The test section was evacuated to 50 torr to minimize aerodynamic heating and deceleration of the rod and yet provide high enough drag to effect aerodynamic separation of the sabot from the larger rod. The gun barrel was evacuated to approximately 50 μ to eliminate heating during the acceleration.

The test sequence begins with the firing of the light gas gun and the acceleration of the rod and sabot down the 6-ft-long, smooth bore gun barrel. Upon leaving the gun barrel, the rod enters the test section where it first passes through the network of small rods. The rod then pierces a trigger grid which fires the x-ray unit and simultaneously starts a chronograph. Subsequently, as the rod proceeds downstream the shadowgraph station is triggered and finally grid three is triggered, stopping the chronograph. A lead target at the end of the test section arrests the rod.

Sabot Development

Throughout the test program, the rod was enclosed in a sabot that fitted into the gun barrel. The purpose of the sabot was to support the rod while in the launch tube and to guide it down the tube. Several of the sabot designs used are shown in Fig. 5. The simplest sabot design used is shown in Fig. 5a. With this design the rod remained attached to the leading edge of the sabot during the impact. Although the sabot functioned as designed, the lack of resolution of the flash x ray or its inability to define the boundaries of the rod, as shown in Fig. 6, produced, at best, marginal results.

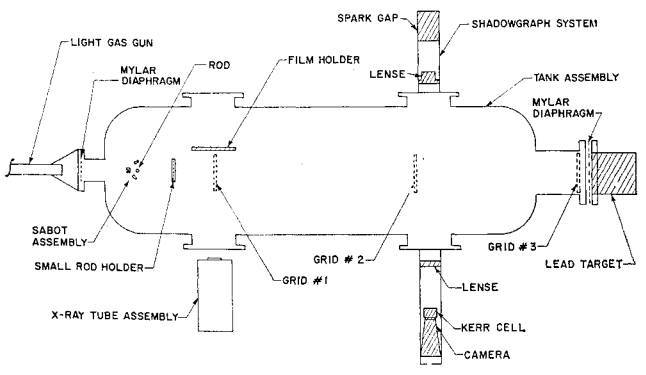

Fig. 4 Schematic of Range II test section.

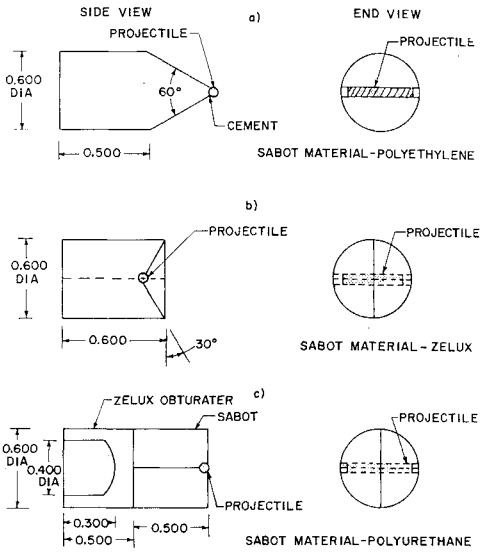

Fig. 5 Drawings of several sabot designs used.

Consequently, a sabot was designed which separated from the rod as soon as it left the launch tube. The initial phase of the sabot development was concerned with finding a material with a high-strength-to-weight ratio and a low density. Polyurethane, having a density of 17.2 lb/ft^3, proved to be adequate for this application.

Once the material was selected, modifications were made to the sabot package to provide the most efficient system (based on ratio of successful to unsuccessful tests), Fig. 5c. The sabot was split into four pieces, thereby reducing the ballistic coefficient of the system, since the pieces are aerodynamically separated once they are in free flight. A hole for containing the rod was drilled through the sabot normal to the axis of symmetry and tangent to the leading edge of the sabot. The sabot was fitted into the barrel with a 0.0002-in. interference to provide positive contact of the sabot with the bore of the launch tube. An obturating plug, Fig. 5c, was placed behind the sabot to isolate it from the high-pressure hydrogen gas. This plug was generally separated by $\frac{1}{4}$ in. from the rod when impact occurred as shown in Fig. 7. Figure 7 is also typical of a data point in which the larger rod is cut. Figure 8, on the other hand, is typical of a datum for which complete cutting did not occur (although very nearly in this case).

Test Result and Discussion

All tests were conducted at a speed of 19,000 fps. The results are given in Table 1. The experimental value of B/A was established for a given system by performing a series of tests which covered a range from complete to partial fracture by making small incremental changes in the ratio of rod diameters. Fractured and unfractured results were indicated by the x radiographs as shown in Figs. 7 and 8. The experimental value of B/A was taken as the arithmetic mean of the two nearest ratios that resulted in fracture and in no fracture. The materials used in the tests were 7075T6

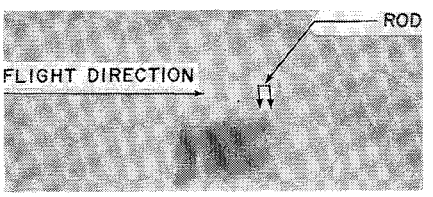

Fig. 6 X-ray showing test using integral sabot design; velocity = 17,500 fps, rod = 0.050-in.-diam aluminum.

Table 1 Experimental results at a relative velocity of 19,000 fps

Larger rod material	Larger rod diameter, in.	Smaller rod material	Smaller rod diameter, in.	Results	Diameter ratio	Experimental B/A	Experimental scale (mean larger rod diameter in in.)	B/A from Eq. (2)	B/A from Eq. (3)	Symbol
Aluminum	0.040	Quartz	0.008	Fracture	5					
Aluminum	0.040	Quartz	0.004	No fracture	10	7.5	0.040	2.1	5.8	○
Aluminum	0.050	Quartz	0.010	Fracture	5					
Aluminum	0.050	Quartz	0.008	No fracture	6.3	5.65	0.050			
Aluminum	0.200	Quartz	0.045	Fracture	4.4					
Aluminum	0.225	Quartz	0.045	No fracture	5.0	4.7	0.212			
Aluminum	0.050	Steel	0.005	Fracture	10					
Aluminum	0.075	Steel	0.005	No fracture	15	12.5	0.067	3.6	10.3	□
Aluminum	0.075	Platinum	0.005	Fracture	15					
Aluminum	0.100	Platinum	0.005	No fracture	20	17.5	0.087	6.0	17.8	△
Titanium	0.030	Steel	0.005	Fracture	6					
Titanium	0.040	Steel	0.005	No fracture	8	7.0	0.035	2.8	7.9	▷
Titanium	0.030	Tungsten	0.003	Fracture	10					
Titanium	0.040	Tungsten	0.003	No fracture	13.3	11.65	0.035	4.4	12.7	▽
Steel	0.030	Tungsten	0.003	No fracture	10					
Steel	0.020	Tungsten	0.003	Fracture	6.7	8.35	0.025	3.4	9.6	◇
Steel	0.050	Tungsten	0.005	No fracture	10					
Steel	0.080	Tungsten	0.010	Fracture	8	9.0	0.065			
Steel	0.160	Tungsten	0.014	Fracture	11.4					
Steel	0.180	Tungsten	0.014	No fracture	12.9	12.15	0.170			

aluminum, 6AL4V titanium, 4340 steel, fused quartz, pure platinum, and pure tungsten.

As discussed in the Introduction, the purpose of our tests was to establish a correlation of the form of Eq. (1). In particular, we wished to know, first, the correct power dependence of B/A upon D, second, if a correlation of the form of Eq. (1) gives generally correct larger rod material dependence, and last, if the ratio B/A is truly independent of the actual scale of the experiment.

Consider the last question first. The smallest diameter larger rod tested during the program was of 0.020-in. diameter. To determine if this was a significant limitation, the fracture ratio B/A was determined experimentally over a five to one scale range for quartz cutting aluminum and over a seven to one scale range for tungsten cutting steel. The results are shown in Table 1. Note that, although there is a slight variation in the experimental B/A in both cases, the variation is small with respect to the scale variation and is, in fact, opposite in sense for the two cases. Thus, it seems reasonable to conclude that the fracture ratio B/A will not be substantially different for, say, a 0.005-in. diam larger rod.

The data summarized in Table 1 may also be used to ascertain the approximate dependence of B/A on the smaller rod density D. This behavior is of interest for two reasons. First of all, the various infinite target models[1–7] differ substantially from each other in their prediction of the dependence of B/A upon D. Secondly, if, as discussed in the Appendix, we wish to minimize the weight of a given smaller rod required to cut the larger, the dependence of the fracture ratio on smaller rod density is quite important. With these questions in mind consider Fig. 9, in which are plotted the experimentally determined B/A for various density smaller rods of approximately the same diameter impacting aluminum and titanium larger rods. The upper, aluminum line has a slope of 0.41 and the lower, titanium line has a slope of 0.56. This suggests that the dependence of B/A upon D is approximately to the $\frac{1}{2}$ power as postulated in Ref. 7. Let us therefore compare our experimental results with the correlation of Ref. 7, namely,

$$B/A = 1.96(D/W)^{1/2}(u/a)^{2/3} \tag{2}$$

This comparison is made in Table 1, in the columns labeled "Experimental B/A" and "B/A from Eq. (2)." Note that, as anticipated, Eq. (2) consistently underpredicts B/A by about a factor of 3. But, what is more important, the results of Eq. (2) predict the relative values of B/A fairly well. This indicates that the experimental data correlate well against the variable $(D/W)^{1/2}$ or one closely related to it. Therefore, let us postulate an empirical correlation, based on Eq. (2) of the form

$$B/A = K(u/a)^{2/3}(D/W)^{J}$$

This may be written alternately as

$$\ln(B/A)(a/u)^{2/3} = \ln K + J \ln(D/W)$$

and a conventional least-square straight-line fit obtained for $\ln(B/A)(a/u)^{2/3}$ as a function of $\ln(D/W)$. This was done for all the data in Table 1 and resulted in the formula

$$B/A = 5.45(u/a)^{2/3}(D/W)^{0.53} \tag{3}$$

with root-mean-square deviation of 1.4. (Note that the u/a dependence remains purely speculative.) This result reinforces the implication drawn from Fig. 9 suggesting an approximately $\frac{1}{2}$ power dependence of B/A upon D. The fact that J is approximately one-half has the following physical interpretation. As shown in the Appendix, this value of J indicates that the mass per unit length of smaller rod required to cut the larger rod is independent of the properties of the smaller rod. This, in turn, means that the mass of

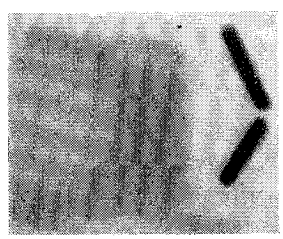

Fig. 7 X-ray showing test using four-piece sabot design and fractured rod, 0.050-in.-diam tungsten.

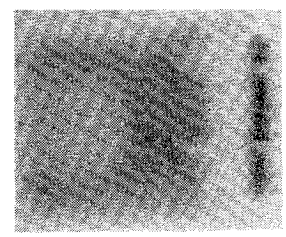

Fig. 8 X-ray showing partially severed rod, 0.050-in.-diam steel.

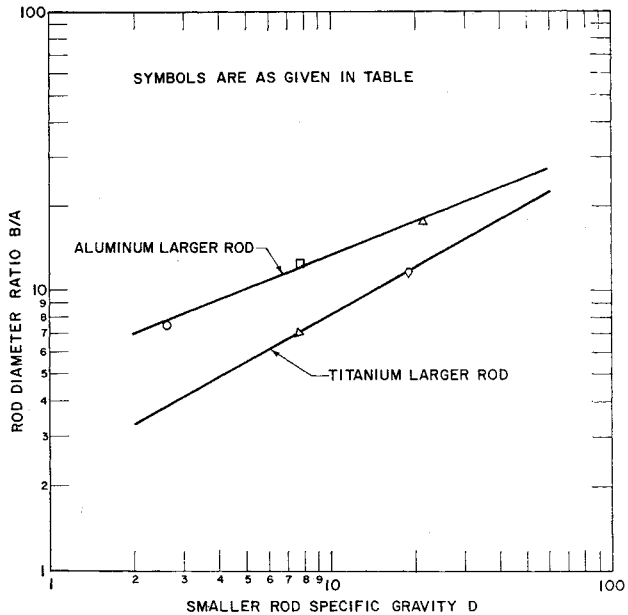

Fig. 9 Graph of B/A vs D for two larger rod materials.

smaller rod swept out in cutting the larger rod is independent of the properties of the small rod.

Appendix

Suppose we wish to determine the minimum weight smaller rod which upon impact at a given speed will break a larger rod of given material and diameter. Since the length of the smaller rod is fixed by the requirement that it intercept the path of the larger rod, the minimum weight smaller rod will simply have the minimum weight per unit length m. This is given by

$$m = \pi DA^2/4$$

But we have from our investigation, as previously indicated,

$$B/A = K(u/a)^{2/3}(D/W)^J$$

Eliminating A between these two equations yields

$$m = (\pi/4)(B/K)^2(a/u)^{4/3}W^{2J}D^{1-2J}$$

Thus, for a given larger rod diameter and material and for a given impact speed, m is proportional to D^{1-2J}. Then if J is greater than $\frac{1}{2}$, we will obtain the minimum weight smaller rod that will cut the larger by making it (the smaller) of the heaviest practical material. This will result, of course, in a small value of A. On the other hand, if J is less than $\frac{1}{2}$, the minimum weight smaller rod will be made of the lightest practical material and will be of correspondingly large diameter A. Finally, if J is equal to, or nearly equal to, $\frac{1}{2}$ the weight per unit length of the smaller rod is fixed and the appropriate combination of D and A can be chosen for other practical reasons.

From this simple analysis, it is clear that if a minimum value of m is important, the dependence of B/A upon D must be known with some exactness.

References

[1] Gehring, J., Meyers, C., and Charest, J., "Experimental Studies of Impact Phenomena and Correlation with Theoretical Models," Proceedings of the Seventh Hypervelocity Impact Symposium, Orlando, Fla., Feb. 1965.

[2] Bjork, R., "Numerical Solutions of the Axially Symmetric Hypervelocity Impact Process Involving Iron," Proceedings of the Third Symposium on Hypervelocity Impact, Chicago, Ill., Feb. 1959.

[3] Hermann, H. and Jones, J., "Survey of Hypervelocity Impact Information," ASRL Rept. 99-2, Oct. 1962, Massachusetts Institute of Technology.

[4] Eichelberger, R. and Gehring, J., "Effects of Meteoroid Impacts on Space Vehicles," *ARS Journal*, Vol. 32, No. 10, Oct. 1962, pp. 1583–1591.

[5] Summers, J. and Charters, A., "High Speed Impact of Metal Projectiles in Targets of Various Materials," Proceedings of Third Symposium on Hypervelocity Impact, Chicago, Ill., Oct. 1958.

[6] Naumann, R., "A Physical Basis for Scaling Hypervelocity Impact," Proceedings of Seventh Hypervelocity Impact Symposium, Orlando, Fla., Feb. 1965.

[7] Bruce, E. P., "Review and Analysis of High Velocity Impact Data," Proceedings of the Fifth Symposium on Hypervelocity Impact, Denver, Colo., Nov. 1961.